Classical analogy of Fano resonances

2006 Phys. Scr. 74 259

(http://iopscience.iop.org/1402-4896/74/2/020)

INSTITUTE OF PHYSICS PUBLISHING PHYSICA SCRIPTA
Phys. Scr. **74** (2006) 259–266 doi:10.1088/0031-8949/74/2/020

Classical analogy of Fano resonances

Yong S Joe[1], **Arkady M Satanin**[1,2] **and Chang Sub Kim**[3]

[1] Centre for Computational Nanoscience, Department of Physics and Astronomy, Ball State University, Muncie, IN 47306, USA
[2] Institute for Physics of Microstructures, RAS, GSP-105, Nizhny Novgorod 603950, Russia
[3] Department of Physics and Institute for Condensed Matter Theory, and Institute of Opto-Electronic Science and Technology, Chonnam National University, Gwangju 500–757, Korea

E-mail: ysjoe@bsu.edu

Received 23 January 2006
Accepted for publication 23 May 2006
Published 19 July 2006
Online at stacks.iop.org/PhysScr/74/259

Abstract
We present an analogy of Fano resonances in quantum interference to classical resonances in the harmonic oscillator system. It has a manifestation as a coupled behaviour of two effective oscillators associated with propagating and evanescent waves. We illustrate this point by considering a classical system of two coupled oscillators and interfering electron waves in a quasi-one-dimensional narrow constriction with a quantum dot. Our approach provides a novel insight into Fano resonance physics and provides a helpful view in teaching Fano resonances.

PACS numbers: 46.40.Ff, 03.65.Nk, 73.23.Ad, 73.63.Kv

1. Introduction

Resonance is a major subject of theoretical and experimental investigation and the concept of resonances is ubiquitous in physics and teaching. The search for new effects related to wave interference and different kinds of resonances in various physical systems may be of interest. Interference of a localized wave with propagating states and resulting Fano resonances in atomic and solid state structures have been attracting much attention recently [1–19]. At present, nanotechnology provides various solid state systems such as Aharonov–Bohm (AB) rings, two-dimensional (2D) electronic waveguides, nanotubes etc, where alternative electronic paths may be realized. When there is one open channel, in particular, for the electrons in a waveguide, the transmission (the dimensionless conductance) can be represented as [19]

$$T(E) = \frac{1}{1+q^2}\frac{(\varepsilon+q)^2}{1+\varepsilon^2}, \qquad (1)$$

where q is the coupling parameter, $\varepsilon = (E - E_R)/\Gamma$ is the reduced energy, and E_R and Γ are the peak position and the width of the resonance, respectively. The parameter q measures quantitatively the asymmetry degree of resonance line in Fano interference between the evanescent bound states and propagating continuum states. If the coupling parameter q becomes very strong ($q \gg 1$), then the Fano profile reduces to a symmetric Breit–Wigner (BW) (or Lorentzian) lineshape. For instance, the BW resonances take place in the transmission of two-barrier heterostructures.

Now it is clear that the Fano interference is a universal phenomenon because the manifestation of configuration interference does not depend on the matter. The natural question then arises: why are Fano-interference phenomena so interesting in different topics of physics? From the practical point of view, for instance, the resonances can be considered as quantum '*probes*' that provide important information on the geometric configuration and internal potential fields of low-dimensional structures. Fano interference may potentially be used for the design of new types of quantum electronic or spintronic devices such as Fano-transistors [12], spin transistors and Fano-filters for polarized electrons [16]. In addition, Fano phenomena can also be used for lasing without population inversion [17]. From the educational point of view, there are wave phenomena such as Young's interference in optics or AB interference in quantum mechanics which are milestones in modern physics. Without a doubt, Fano interference is such a phenomenon. It is shown that BW resonances arise due to the interference of two counter waves in the same scattering channel (similar to resonances of the Fabry–Perot interferometre in optics). On the other hand, Fano resonances take place due to wave interference in different channels.

The main purpose of the present work is to give an intuitive explanation of the physical nature of Fano resonances.

We begin by introducing the basic ideas of the resonance manifestation in simple mechanical systems by considering a single oscillator system. The following coupled oscillator model provides the main idea about the analytical zero-pole structure of the amplitude and phase behaviours near the resonances. As a consequence, we obtain the physical meaning of the amplitude-zero in these systems. Next, we examine the Fano interference in quantum systems and give a detailed analysis of the phenomena in a quantum constriction with an embedded attractive potential (a quantum dot). In doing so, we find that an interpretation of the manifestation of Fano interference in quantum structures analogous to coupled classical oscillators is interesting and useful.

2. Resonance in harmonic oscillator systems driven by an external force

2.1. A single oscillator

We first consider an oscillating motion in a single oscillator. We briefly recall the behaviour of the single mechanical oscillator in a medium under an external harmonic force. Thus, if a particle moves under the combined influence of a linear restoring force, a resisting force, and an external driving force, then the differential equation that describes the motion is

$$\ddot{x} + \gamma\dot{x} + \omega_0^2 x = A\cos\omega t, \tag{2}$$

where ω_0 is the natural frequency (eigenmode) of the oscillator in the absence of damping (defined by the mass and the spring constant), γ is a frictional parameter, and ω is a frequency of the external force. The general solution of equation (2) is the sum of the complementary x_c and the particular x_p solutions. The complementary solution describes the motion of a damping oscillator

$$x_c(t) = e^{-\gamma t/2}[q_1 e^{i\Omega t} + q_2 e^{-i\Omega t}], \tag{3}$$

where $\Omega = \sqrt{{\omega_0}^2 - \gamma^2/4}$, and q_1 and q_2 are complex amplitudes ($q_1 = q_2^*$).

The simple way of finding a particular solution of equation (2) is to use the complex representation. To this end, we rewrite the equation (2) for a particular solution x_p as

$$\ddot{x}_p + \gamma\dot{x}_p + \omega_0^2 x_p = \tfrac{1}{2}A(e^{i\omega t} + e^{-i\omega t}). \tag{4}$$

The solution may be written as $x_p = x^+ + x^-$, where $x^\pm$ are solutions for the 'positive' and the 'negative' frequencies, respectively. Thus, the particular solutions can be written as $x_p(t) = 2\mathrm{Re}(x^+(t))$, where x^+ may be considered as the solution of the equation

$$\ddot{x}^+ + \gamma\dot{x}^+ + \omega_0^2 x^+ = a e^{i\omega t}, \tag{5}$$

and $a = A/2$. Now, the solution of equation (5) can be expressed in a complex form as $x^+(t) = c e^{i\omega t}$. Here, the complex amplitude $c(\omega)$ takes the form as

$$c(\omega) = \frac{a}{\omega_0^2 - \omega^2 + i\gamma\omega}, \tag{6}$$

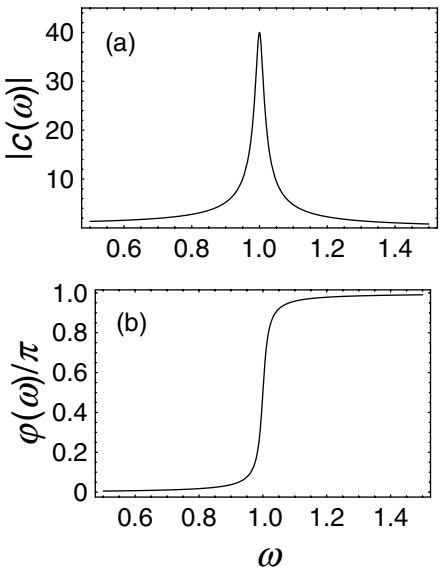

Figure 1. (a) The resonant behaviour of the amplitude in the single, driven oscillator as a function of the frequency; where the frequency of the oscillator is in units of the natural frequency, ω_0. (b) The phase jump by π near the resonance is shown. (Here, a frictional parameter $\gamma = 0.025$ is used, and the amplitude is in units of a/ω_0^2).

and has the modulus $|c(\omega)|$ and the phase $\varphi(\omega) : c(\omega) = |c(\omega)|e^{-i\varphi(\omega)}$, where

$$|c(\omega)| = \frac{a}{\sqrt{(\omega_0^2 - \omega^2)^2 + \omega^2\gamma^2}}, \qquad \varphi(\omega) = \tan^{-1}\left(\frac{\omega\gamma}{\omega_0^2 - \omega^2}\right). \tag{7}$$

When we consider the steady-state effects ($t \gg \gamma^{-1}$), the complementary solution gives a small correction and then can be neglected. In this case, the solution has the form

$$x(t) \approx |c(\omega)|\cos[\omega t - \varphi(\omega)]. \tag{8}$$

We assume here that the inequality $\gamma \ll \omega_0$ holds for the oscillator parameters. In figure 1(a), it is shown that a resonance in $|c(\omega)|$ occurs as the frequency ω of the external force approaches to the natural frequency ω_0 of the oscillator. At the resonance the amplitude of the oscillator takes the value of $|c(\omega_0)| \approx a/\omega_0\gamma \gg |c(0)|$. We can see from equation (7) that the phase of the oscillator changes by π when the frequency ω goes through the resonance (see figure 1(b)). This indicates that there is a delay between the action of the driving force and the response of the oscillator. As ω increases, the phase increases from $\varphi = 0$ at $\omega = 0$ to $\varphi = \pi/2$ at $\omega = \omega_0$ (at resonance) and to π as $\omega \to \infty$. It means that if the displacement and the external force are in phase before the resonance, then they are out of phase after the resonance.

2.2. Two coupled oscillators

Now we discuss the dynamics of a pair of classical oscillators coupled by a weak spring. Since we are interested in the behaviour of the amplitudes after the transient motion decays, we may well consider only the particular solution by neglecting a complementary solution. We have seen in the previous section that the resonant properties are defined

by complex amplitudes. The equations of motion may be written as

$$\ddot{x}_1 + \gamma_1\dot{x}_1 + \omega_1^2 x_1 + v_{12}x_2 = a_1 e^{i\omega t},$$
$$\ddot{x}_2 + \gamma_2\dot{x}_2 + \omega_2^2 x_2 + v_{12}x_1 = 0, \tag{9}$$

where v_{12} describes the coupling of the oscillators.

Firstly, we review the free motion of oscillators ($a_1 = 0$). In the absence of the coupling ($v_{12} = 0$), the two free oscillators swing independently with the given natural frequencies. On the other hand, the coupled oscillators have two normal modes (or eigenmodes): firstly, two oscillators swing back and forth together; secondly, they move in opposite directions. In order to understand the meaning of eigenmodes, let us assume that there are no frictions of the oscillators, $\gamma_1 = \gamma_2 = 0$. Then, the eigenmodes of the coupled oscillators can be obtained from

$$(\omega_1^2 - \omega^2)(\omega_2^2 - \omega^2) - v_{12}^2 = 0. \tag{10}$$

If the coupling parameter is weak ($\omega_2^2 - \omega_1^2 \gg v_{12}$), then the eigenmodes of coupled system can be written as

$$\tilde{\omega}_1^2 \approx \omega_1^2 - \frac{v_{12}^2}{\omega_2^2 - \omega_1^2}, \qquad \tilde{\omega}_2^2 \approx \omega_2^2 + \frac{v_{12}^2}{\omega_2^2 - \omega_1^2}, \tag{11}$$

which are slightly shifted from the eigenmodes of independent oscillators in the real axis.

Next, we consider the general problem of the excited oscillators given in equation (9) with friction. After some manipulation, one can obtain that the steady-state solutions for the displacement of the oscillators are also harmonic such that

$$x_1 = c_1 e^{i\omega t}, \qquad x_2 = c_2 e^{i\omega t}. \tag{12}$$

Here, the amplitudes have the forms

$$c_1 = \frac{(\omega_2^2 - \omega^2 + i\gamma_2\omega)}{(\omega_1^2 - \omega^2 + i\gamma_1\omega)(\omega_2^2 - \omega^2 + i\gamma_2\omega) - v_{12}^2} a_1, \tag{13}$$

$$c_2 = -\frac{v_{12}}{(\omega_1^2 - \omega^2 + i\gamma_1\omega)(\omega_2^2 - \omega^2 + i\gamma_2\omega) - v_{12}^2} a_1. \tag{14}$$

The phases of the oscillators are defined through

$$c_1(\omega) = |c_1(\omega)|e^{-i\varphi_1(\omega)}, \qquad c_2(\omega) = |c_2(\omega)|e^{-i\varphi_2(\omega)}. \tag{15}$$

Note that the phase difference between two oscillators is given by

$$\varphi_2 - \varphi_1 = \pi - \theta,$$

where the extra phase shift θ is defined by the numerator of equation (13) as

$$\theta = \tan^{-1}\left(\frac{\gamma_2\omega}{\omega_2^2 - \omega^2}\right). \tag{16}$$

Let us analyse, in detail, the case when the frictional parameter of the second oscillator is equal to the zero ($\gamma_2 = 0$). It is clear that the coupled system has an effective friction for normal modes, which means that the amplitudes of the oscillators are limited. The amplitude of the first oscillator as a function of the frequency of an external force is shown in figure 2(a), where we have used $\gamma_1 = 0.025$ and $v_{12} = 0.1$.

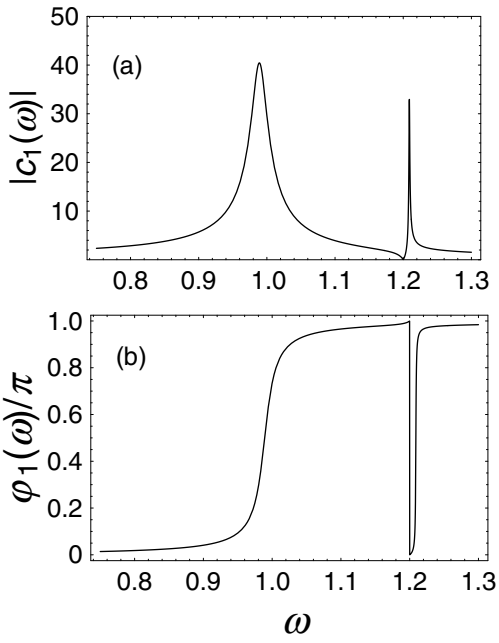

Figure 2. (a) The resonant behaviour of the amplitude of the first oscillator in the coupled system; where the frequency is in units of the natural frequency ω_1. The amplitude has two peaks (symmetric and asymmetric line-shape) near the eigenfrequencies $\omega = \mathrm{Re}[\tilde{\omega}_1] = 1.0$ and $\omega = \mathrm{Re}[\tilde{\omega}_2] = 1.21$ and it vanishes at the zero-frequency, $\omega = \omega_{zero} = 1.2$. (The modulus of the amplitude is in units of a/ω_0^2.) (b) The phase behaviour of the first oscillator amplitude around the resonances.

Two resonant peaks appear in the chosen frequency windows: one symmetric at $\omega \approx 1$ and the other asymmetric at $\omega \approx 1.21$. The location of the resonant peaks corresponds to the real parts of the complex eigen-frequencies, $\tilde{\omega}_1$ and $\tilde{\omega}_2$, which are determined from the vanishing condition of the denominator of equations (13) and (14). The imaginary part of the eigen-frequency specifies the width of the resonance, so as the single oscillator case. The reason why the second resonant peak is asymmetric is due to existence of the zero-frequency at $\omega_{\mathrm{zero}} = \omega_2 = 1.2$ which is right near the peak position. It can be seen from equation (13) that the amplitude of the first oscillator c_1 becomes zero at $\omega = \omega_2$ when $\gamma_2 = 0$. Accordingly, the line shape of the second resonance becomes distorted. Note that the amplitude of the second oscillator c_2 tends to a_1/v_{12} in equation (14) at the zero-frequency.

Now we attempt to understand the physical meaning of the amplitude-zero in the first oscillator by closely examining figures 2 and 3. Because there is a coupling between the first and second oscillators, the phases of both oscillators are changed when the driving frequency passes through the resonances. In order to analyse the behaviour of phase, we sweep the frequency of an external force starting from a value below the first resonant mode. It means that both the first and second oscillators are being driven by the frequency of an external force that is less than the resonant frequencies ($\omega < \mathrm{Re}[\tilde{\omega}_1] = \omega_1$, $\mathrm{Re}[\tilde{\omega}_2] = 1.21\omega_1$). When the first oscillator is being driven near the resonance ($\omega \leqslant \mathrm{Re}[\tilde{\omega}_1]$), the amplitude quickly grows to a maximum in figure 2(a) and the displacement x_1 of the first oscillator gets the phase $\pi/2$ right across the resonance as seen in figure 2(b). After the frequency passes through the first resonance, but

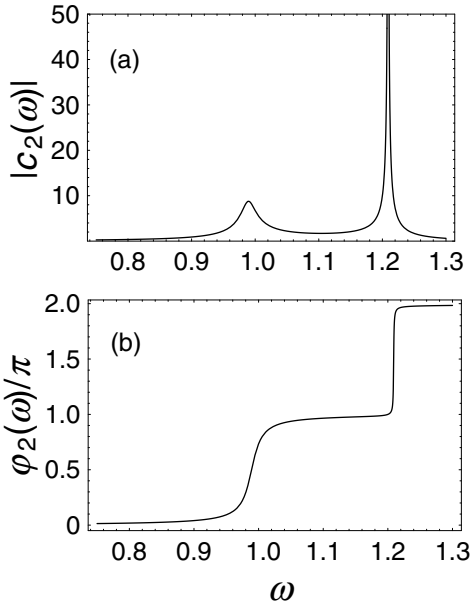

Figure 3. (a) The amplitude of the second oscillator as a function of the frequency; where the frequency is in units of ω_1. Two symmetric, resonant peaks appear at the eigenmodes of the coupled oscillators. (The modulus of amplitude is in units of a/ω_0^2.) (b) The phase behaviour of the second oscillator; where a sequential phase change by π is seen as the driving frequency passes through the resonances.

before it meets the zero-frequency ω_{zero}, the first oscillator settles into steady-state motion (i.e., the transient motion has already decayed) and the displacement x_1 is eventually π out of phase with respect to the external force. Next, as the frequency passes through the anti-resonance at $\omega = \omega_{\text{zero}}$, the phase of the oscillator drops by π abruptly. Finally, when the frequency sweeps through the second resonance, the oscillator gains the phase factor by π.

The tendency of the resonance and of the phase of the second oscillator as a function of the frequency is rather straightforward and the results are shown in figure 3. Two resonant peaks appear and they manifest the symmetric line shapes in figure 3(a). In figure 3(b), the phase gain of the second oscillator by π is clearly seen at each time when the frequency passes through the resonances. Focusing on the behaviour of the coupled amplitudes at the zero-frequency, we find that the first oscillator is out of phase with the second oscillator as ω goes through ω_{zero} and that, at this particular frequency, the motion of the first oscillator is quenched enforced *effectively* by the second oscillator.

We have also studied the situation when the frictional coefficient γ_2 is not strictly zero, but finite. In this case, the amplitudes of the first and second oscillators are influenced by the presence of γ_2. We have seen that the amplitudes of both the asymmetric line-shape resonance in $|c_1(\omega)|$ from equation (13) and the symmetric line-shape resonance in $|c_2(\omega)|$ from equation (14) become smaller as γ_2 increases (not shown here). In addition, the zero-frequency of the first oscillator is shifted to the complex-energy plane, accordingly the amplitude does not vanish at the zero-frequency but gains a small value.

Further, we find that the zero-frequency of the amplitude depends on the model we consider. When we generalize the previous treatment to three coupled oscillators, or more, and when only nearest-neighbour couplings are considered, v_{12} and v_{23}, we obtain that the zero-frequency of the amplitude of the first oscillator is defined by the equation

$$(\omega_2^2 - \omega^2)(\omega_3^2 - \omega^2) - v_{23}^2 = 0 \tag{17}$$

(Here, we have considered the case when $\gamma_1 = \gamma_2 = \gamma_3 = 0$.) If $\omega_3 \gg \omega_2$, the zero-frequency ω_{zero} for three coupled oscillators can be expressed as

$$\omega_{\text{zero}}^2 \approx \omega_2^2 - \frac{v_{23}^2}{\omega_3^2 - \omega_2^2}. \tag{18}$$

This indicates that the position of the amplitude-zero differs from the previous value of ω_2 and is shifted in the real energy axis due to the interaction among the oscillators.

3. Fano resonance in a 2D electron waveguide with an attractive potential (quandum dot)

There is an analogy between the classical system of the coupled oscillators, which we have investigated in section 2, and a system of the coupled waves in an electronic waveguide. In order to see the connection between an asymmetric line-shape near the resonant frequency in the coupled oscillators and a main feature of the Fano phenomenon associated with the propagating and evanescent waves in a quantum system, we study propagation of the electron waves in an electronic 2D waveguide of width W arranged along the x-axis. The waveguide geometry is schematically depicted in figure 4, showing a potential region and an attractive quantum dot (grey-coloured area) in the waveguide. Here, the confining potential in the transverse direction is characterized by the function $V_c(y)$ and the attractive potential (dot) by the function $V(x, y)$. There is a complete basis of functions describing the transverse motion $\phi_n(y)$ of an electron with energies, $E_n = \hbar^2\pi^2 n^2/2mW^2$ (with the effective mass m). The electron waves in the perfect waveguide stretched to infinity are described by a combination of the plane wave along the longitudinal direction and confined wavefunctions in the transverse direction such as $e^{\pm ik_n x}\phi_n(y)$, where a wave vector along the x-direction $k_n = \sqrt{2m(E - E_n)}/\hbar$ and n is the number of transverse state. Those propagating states can be considered as open channels in the waveguide.

In order to find wavefunction of electron in a waveguide with the dot, we solve the 2D Schrödinger equation

$$\begin{aligned} &-\frac{\hbar^2}{2m}\left(\frac{\partial^2}{\partial x^2} + \frac{\partial^2}{\partial y^2}\right)\Psi(x, y) \\ &+ V_c(y)\Psi(x, y) + V(x, y)\Psi(x, y) \\ &= E\Psi(x, y), \end{aligned} \tag{19}$$

with the plane wave boundary conditions in leads ($x \to \pm\infty$). It is convenient to expand the wavefunction in the complete basis of functions describing the transverse motion

$$\Psi(x, y) = \sum_{n=1}^{\infty} \psi_n(x)\phi_n(y). \tag{20}$$

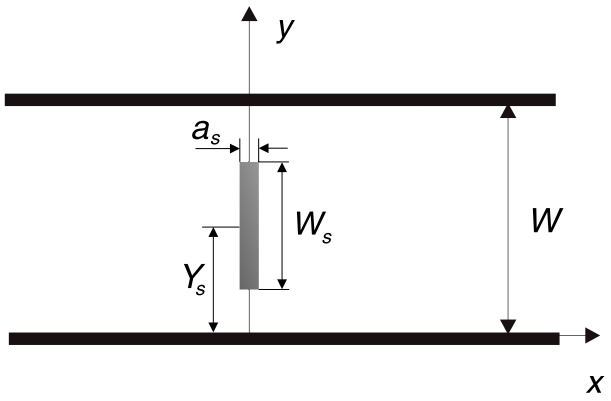

Figure 4. Schematic illustration of the electron waveguide with an embedded quantum dot (grey-coloured area); where the attractive potential well is centred at $x = 0$ and $y = Y_s$ and the electron motion is not limited horizontally, $-\infty < x < \infty$, but is confined vertically, $0 < y < W$.

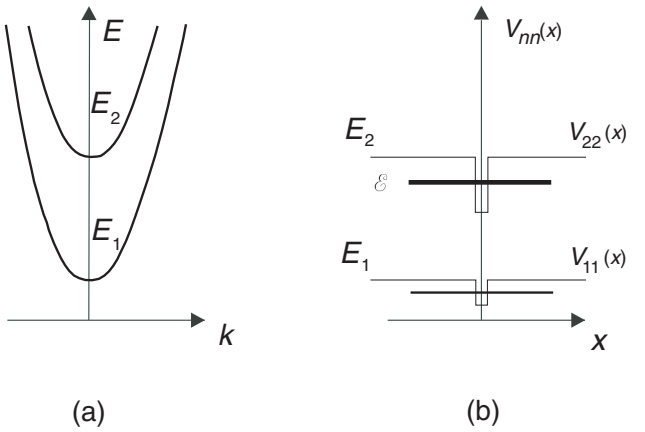

Figure 5. (a) Energy dispersion relation for an electron in a perfect waveguide and (b) the diagrams for a bound level (near the first sub-band) and quasi-bound level (near the second sub-band) in the dot's effective potential.

Substituting equation (20) into equation (19), we obtain the coupled-channel equations for an electron in the form

$$-\frac{\hbar^2}{2m}\frac{\partial^2}{\partial x^2}\psi_n(x) + \sum_{n'=1}^{\infty} V_{nn'}(x)\psi_{n'}(x) = (E - E_n)\psi_n(x), \tag{21}$$

where the coupling matrix elements of the dot's potential (which still acts on the x coordinate) are defined to be

$$V_{n\,n'}(x) = \int \phi_n(y)V(x, y)\phi_{n'}(y)\,\mathrm{d}y. \tag{22}$$

Since equation (21), which is equivalent to the 2D Schrödinger equation, cannot be solved in general, we use some simplification that allows us to use a resonant perturbation theory [20, 21] in the system under the investigation.

We model the scattering potential as a thin rectangular potential-well by assuming that the longitudinal size of the potential well is much smaller than the characteristic wavelengths of the electron. Then, the matrix elements of the potential can be written as

$$V_{nn'}(x) = -\frac{\hbar^2}{m}v_{nn'}\delta(x), \tag{23}$$

where the parameters $v_{nn'}$ of the dot are expressed in an explicit form [11]. It can be shown that the short range potential provides the following boundary conditions to be imposed on the multi-component wavefunctions at $x = 0$

$$\begin{aligned} \psi_n(0+) &= \psi_n(0-), \\ \psi_n'(0+) - \psi_n'(0-) &= -2\sum_{n'=1}^{\infty} v_{nn'}\psi_{n'}(0\pm). \end{aligned} \tag{24}$$

Here, we consider the situation when the energy of incoming electron is placed in the interval $E_1 < E < E_2$ (the first energy window), as shown schematically in figure 5. If the characteristic value of matrix element V_{12}, describing the coupling between two nearest channels, is small compared to the sub-band distance, then we only need to consider two coupled equations in the first energy window to understand the main physical features of the interference. It is well known that the remaining modes in the waveguide with the attractive impurity only alter the width and position of the resonances and hence play a minor role in the Fano phenomenon. Without much difficulties, our formulation can be extended for a multi-band approximation.

The wavefunction in the first channel, obtained from the solutions of the Schrödinger equation, can be written as

$$\psi_1(x) = \begin{cases} a_1 \mathrm{e}^{\mathrm{i}k_1 x} + b_1 \mathrm{e}^{-\mathrm{i}k_1 x}, & x < 0, \\ c_1 \mathrm{e}^{\mathrm{i}k_1 x}, & x > 0, \end{cases} \tag{25}$$

where $k_1 = \sqrt{2m(E - E_1)}/\hbar$ is a wave vector in the first channel. Similarly, the wavefunction in the second channel as

$$\psi_2(x) = \begin{cases} b_2 \mathrm{e}^{|k_2|x}, & x < 0, \\ c_2 \mathrm{e}^{-|k_2|x}, & x > 0, \end{cases} \tag{26}$$

where $|k_2| = \sqrt{2m(E_2 - E)}/\hbar$. Notice that the wavefunction ψ_2 in the second channel is evanescent wave. These two waves interfere in the waveguide and the quantum dot plays a role of a mixer of two different types of waves. The undetermined amplitudes appearing in equations (25) and (26) are specified by applying the matching conditions given in equation (24). Consequently, we obtain

$$\begin{aligned} (\mathrm{i}k_1 + v_{11})c_1 + v_{12}c_2 &= \mathrm{i}k_1 a_1, \\ v_{12}c_1 + (-|k_2| + v_{22})c_2 &= 0, \end{aligned} \tag{27}$$

which give

$$c_1 = \frac{\mathrm{i}k_1(-|k_2| + v_{22})}{(\mathrm{i}k_1 + v_{11})(-|k_2| + v_{22}) - v_{12}^2}a_1, \tag{28}$$

$$c_2 = -\frac{\mathrm{i}k_1 v_{12}}{(\mathrm{i}k_1 + v_{11})(-|k_2| + v_{22}) - v_{12}^2}a_1. \tag{29}$$

From equation (28) the transmission and reflection amplitudes in the first channel are obtained as

$$t_{11} = \frac{c_1}{a_1} = \frac{\mathrm{i}k_1(-|k_2| + v_{22})}{(\mathrm{i}k_1 + v_{11})(-|k_2| + v_{22}) - v_{12}^2}, \tag{30}$$

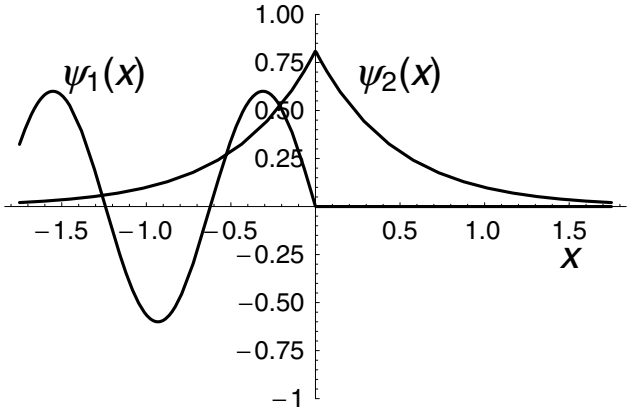

Figure 6. The wavefunctions of the first and second channels when the electron energy matches with the zero-energy. Note that in this case a full reflection occurs.

and

$$r_{11} = \frac{b_1}{a_1} = \frac{-v_{11}(-|k_2| + v_{22}) + v_{12}^2}{(\mathrm{i}k_1 + v_{11})(-|k_2| + v_{22}) - v_{12}^2}, \tag{31}$$

respectively. As it follows from equation (30), the transmission amplitude may vanish if $-|k_2| + v_{22} = 0$. When this happens, the reflection amplitude r_{11} is -1 and the energy at which the transmission becomes zero is determined to be

$$E_{\mathrm{zero}} = E_2 - \frac{\hbar^2 v_{22}^2}{2m}. \tag{32}$$

There is a full reflection of the electron wave from a quantum dot when the electron energy is equal to the zero-energy E_{zero}. The wavefunctions in the first and second channels are schematically depicted in figure 6 at the zero-energy. Like the classical system, we notice that the position of the amplitude-zero depends on the number of the channels. For instance, if we take into account another closed channel $n = 3$ by a perturbation, the zero-energy given by equation (32) is shifted in the real axis of energy, as illustrated in the three coupled oscillators see equation (18). In the meantime, there is a full transmission of the electron wave through the quantum dot when the reflection amplitude $r_{11} = 0$. If we impose $r_{11} = 0$ in equation (31), we get the condition for the reflection-zero, $v_{11}(-|k_2| + v_{22}) - v_{12}^2 = 0$. A real solution to this condition exists at the energy E_{max}

$$E_{\mathrm{max}} = E_2 - \frac{\hbar^2}{2m}\left(v_{22} - \frac{v_{12}^2}{v_{11}}\right)^2. \tag{33}$$

Note that the above expressions (equations (32) and (33)) for the transmission-zero and the reflection-zero energies are exact in the framework of two channel approximation.

We have performed a numerical calculation of the transmission using the following parameters of the waveguide and a quantum dot. The width of the waveguide is set to $W = 23.7\,\mathrm{nm}$ and the $GaAs$ effective mass is used as $m = 0.067 m_0$. This gives $E_1 = 10\,\mathrm{meV}$ and $E_2 = 40\,\mathrm{meV}$ for the first two energy levels due to transverse confinement in the waveguide. The parameters of the quantum dot are as follows: $Y_s = 0.55W$ (the position of the dot in the waveguide), $W_s = 0.5W$ (W_s is the transverse width of the dot), and the scattering

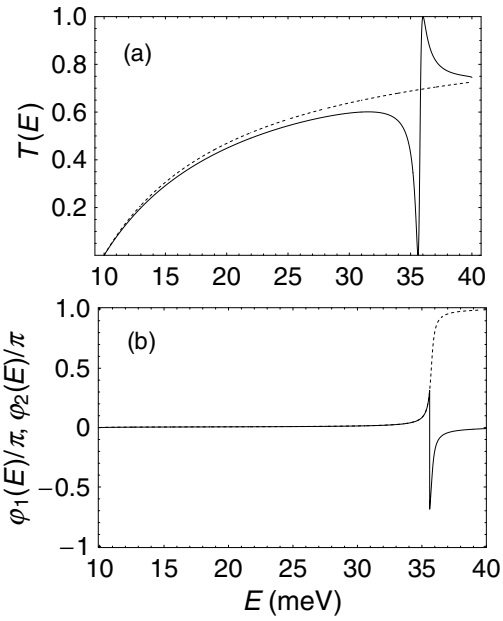

Figure 7. (a) Fano resonance in the transmission for a quantum waveguide with a short-range attractive potential (solid line) and a background transmission (dotted line). (b) The phase shift of the amplitude for the electron wave in the first propagating channel (solid line) and the second evanescent channel (dotted line).

parameters $a_s V_s = 0.1\,\mathrm{eV\,nm}$, where $V_s = 100\,\mathrm{meV}$ (V_s is a depth of attractive potential well) and $a_s = 1\,\mathrm{nm}$ (a_s is a thickness of the potential well). The computed transmission of the system,

$$T(E) = |t_{11}(E)|^2,$$

is plotted in figure 7(a) for the chosen energy window, where for numerical purposes the following characteristic energies for the matrix elements of the potential are used: $\hbar^2 v_{11}^2/2m \cong 11.33\,\mathrm{meV}$, $\hbar^2 v_{22}^2/2m \cong 4.40\,\mathrm{meV}$ and $\hbar^2 v_{12}^2/2m \cong 0.34\,\mathrm{meV}$. The pronounced Fano resonant structure (solid line) is clearly shown, i.e. the combined anti-resonance at $E_{\mathrm{zero}} = 35.60\,\mathrm{meV}$ and the nearby resonance peak at $E_R = 36.01\,\mathrm{meV}$ where the width of resonance line is $\Gamma = 0.19\,\mathrm{meV}$. Notice that if we put our quantum dot at the centre of the waveguide ($v_{12} = 0$), then the interference vanishes and the potential scattering takes place. In this case, only the so-called background profile in the transmission may be seen. This background transmission is also plotted for comparison in figure 7(a) as a dotted line. In figure 7(b), we also show the phase shift of the transmitted electron wave with respect to the incoming wave as a function of the electron energy for the first propagating channel (solid line) and the second evanescent channel (dotted line). One can see that the phase ϕ in the propagating channel changes by π abruptly at the zero-energy and that it jumps up around the resonance peak, thus gaining essentially no net phase shift after passing through the zero-pole structure. On the other hand, the phase ϕ_2 of the evanescent channel changes by π rather smoothly over the anti-resonance and resonance structure. We note that the amplitudes of the transmitted and reflected electron waves in the quantum channels, equations (28) and (29), resemble closely with the amplitudes of the coupled classical oscillators, equations (13) and (14). This indicates that an

analogy is possible between the classical oscillators and the quantum waveguide. Accordingly, we believe that our argument on the physical meaning of the zero-frequency and the phase behaviour associated with the classical system would provide a further insight into the Fano resonance physics. The transmission-zero in the Fano resonance structure in quantum systems corresponds to the situation when the motion of one of the coupled classical oscillators is quenched at a special exciting frequency. In addition, the two systems share a common phase property. The phase drop by π occurs when the electron energy (driving frequency) passes through the special energy (zero-frequency), and the phase jump by π occurs when they pass through the resonant peaks.

To obtain a simple expression for the transmission amplitude near a zero-pole region, we consider the system in the weak coupling regime (i.e. v_{12} is assumed to be small in equation (30)). Expanding the numerator and denominator of equation (30) around the zero and the pole, respectively, one can write the transmission amplitude t_{11} in the desired form

$$t_{11}(E) \sim \frac{E - E_{\text{zero}}}{E - E_R + \mathrm{i}\Gamma}, \tag{34}$$

where E_{R} and Γ are the peak position and the width of the resonance, and E_{zero} is the zero-energy of the resonance. After performing a perturbation approximation we obtain that the real part of the resonance pole can be written as $E_R = E_{\text{zero}} + \delta$, where $\delta = \hbar^2 v_{12}^2 v_{11} v_{22}/m(k_1^2 + v_{11}^2)$ and the width $\Gamma = \hbar^2 v_{12}^2 k_1 v_{22}/m(k_1^2 + v_{11}^2)$. (The energy appearing in k_1 is taken at $E = E_R$.) Here, we note that one can neglect the difference between E_{max} and E_{R} in the weak coupling limit. Furthermore, the expression for the transmission, equation (34), can be cast into the canonical Fano form of equation (1). The coupling parameter q ($q = v_{11}/k_1$ in our perturbation approximation) measures an asymmetry degree of the Fano resonance line shape between the localized states and the continuum states.

The Fano profile and phase shift can be measured when a quantum wire (or waveguide) with an embedded dot is realized as an arm of AB interferometre. In fact, this kind of experimental work has already been performed by Kobayashi *et al* [14] where the phase shift has been investigated. Notice that the arguments discussed in the present work result in the correct reflection on the amplitude–phase behaviour of the conductance of AB interferometer.

4. Summary

We have discussed an analogy between the coupled classical oscillators and the two interfering electron waves in the quantum waveguide with an embedded attractive well. In the mechanical systems of the coupled oscillators under the external harmonic force, we have demonstrated that the Fano-analogous asymmetric resonance line shape can occur in the displacement field. In particular, we have provided a physical meaning of the amplitude-zero by examining the analytical zero-pole structure of the amplitude and the behaviour of the phase near the resonances. At zero-frequency, the oscillating motion of one of the oscillator is quenched, while the other synchronizes with the external driving. In the case of the quantum system, we have shown that the Fano resonance structure in the transmission appears due to the interference between a propagating wave and an evanescent wave. Therefore, the quantum system may be considered as a bound oscillator of the evanescent mode coupled with the oscillator of the propagating mode. In general, the zero-frequency in the classical system (the zero-energy in the quantum system) is complex, and when this happens, instead of the exact quenching, the classical amplitude (the electron transmission) will manifest a small dip. Finally, we remark that Fano interference is a universal phenomenon in the sense that the manifestation of configuration interference does not depend on matter.

Acknowledgments

This work is supported by the Indiana 21st Century Research and Technology Fund. The work of CSK was supported by the special research fund of Chonnam National University in 2004. The work of AMS was supported in part by the Russian Basic Research Foundation grant no. 05–02-16762.

References

[1] Fano U 1961 Effects of configuration interaction on intensities and phase shifts *Phys. Rev.* **124** 1866–78

[2] Breit G and Wigner E 1936 Capture of slow neutrons *Phys. Rev.* **49** 519–31

[3] Adair R K, Bockelman C K and Peterson R E 1949 Experimental corroboration of the theory of neutron resonance scattering *Phys. Rev.* **76** 308

[4] Fano U and Rau A R P 1986 *Atomic Collisions and Spectra* (Orlando, FL: Academic)

[5] Cerdeira F, Fjeldly T A and Cardona M 1973 Effect of free carriers on zone-centre vibrational modes in heavily doped *p*-type Si. II. Optical Modest *Phys. Rev.* B **8** 4734–45

[6] Faist J, Capasso F, Sirtori C, Wes K W and Pfeiffer L N 1997 Controlling the sign of quantum interference by tunnelling from quantum wells *Nature (London)* **390** 589

[7] Tekman E and Bagwell P F 1993 Fano resonances in quasi-one-dimensional electron waveguides *Phys. Rev.* B **48** 2553–9

[8] Gurvitz S A and Levinson Y B 1993 Resonant reflection and transmission in a conducting channel with a single impurity *Phys. Rev.* B **47** 10578–87

[9] Nöckel J U and Stone A D 1994 Resonance line shapes in quasi-one-dimensional scattering *Phys. Rev.* B **50** 17415–32

[10] Zhi-an Shao, Porod W and Lent C S 1994 Transmission resonances and zeros in quantum waveguide systems with attached resonators *Phys. Rev.* B **49** 7453–65

[11] Kim C S, Satanin A M, Joe Y S and Cosby R M 1999 Resonant tunneling in a quantum waveguide: effect of a finite-size attractive impurity *Phys. Rev.* B **60** 10962–70

[12] Göres J, Goldhaber-Gordon D, Heemeyer S, Kastner M A, Shtrikman H, Mahalu D and Meirav U 2000 Fano resonances in electronic transport through a single-electron transistor *Phys. Rev.* B **62** 2188–94

[13] Kim C S, Roznova O N, Satanin A M and Shtenberg V B 2002 Interference of quantum states in electronic waveguides with impurities *JETP* **94** 992–1007

[14] Kobayashi K, Aikawa H, Katsumoto S and Iye Y 2002 Tuning of the Fano effect through a quantum dot in an

Aharonov–Bohm interferometer *Phys. Rev. Lett.* **85** 256806–10

[15] Keyser U F, Borck S, Haug R J, Bichler M, Abstreiter G and Wegscheider W 2002 Aharonov–Bohm oscillations of a tunable quantum ring *Semicond. Sci. Technol.* **17** L22–4

[16] Song J F, Ochiai Y and Bird J P 2003 Fano resonances in open quantum dots and their application as spin filters *Appl. Phys. Lett.* **82** 4561–3

[17] Nikonov D E, Imamoglu A and Scully M O 1999 Fano interference of collective excitations in semiconductor quantum wells and lasing without inversion *Phys. Rev.* B **59** 12212–5

[18] Bandopadhyay S, Dutta-Roy B and Mani H S 2004 Understanding the Fano resonace through toy models *Am. J. Phys.* **72** 1501–07

[19] Rau A R P 2004 Perspective on the Fano resonance formula *Phys. Scr.* **69** C10–C13

[20] Feshbach H 1958 Unified theory of nuclear reactions *Ann. Phys. (NY)* **5** 357–90

[21] Goldberg M and Watson K 1964 *Collision Theory* (New York: Wiley)